ACS APPLIED NANO MATERIALS

www.acsanm.org

Article

Oxygen Nanobubbles-Embedded Hydrogel as Wound Dressing to Accelerate Healing

Wen Ren, Victoria Messerschmidt, Michael Tsipursky, and Joseph Irudayaraj*

Cite This: *ACS Appl. Nano Mater.* 2023, 6, 13116−13126

Read Online

ACCESS | Metrics & More | Article Recommendations | Supporting Information

ABSTRACT: Herein, we propose an oxygen nanobubbles-embedded hydrogel (ONB-G) with carbopol for oxygenation of wounds to accelerate the wound healing process. We integrate carbopol, hydrogel, and dextran-based oxygen nanobubbles (ONBs) to prepare ONB-G where ONBs can hold and release oxygen to accelerate wound healing. Oxygen release tests showed that the proposed ONB-G could encapsulate oxygen in the hydrogels for up to 34 days; meanwhile, fluorescence studies indicated that the ONB-G could maintain high oxygen levels for up to 4 weeks. The effect of carbopol concentration on the oxygen release capacity and rheological features of the ONB-G were also investigated along with the sterility of ONB-G. HDFa cell-based studies were first conducted to evaluate the viability, proliferation, and revival of cells in hypoxia. Scratch assay and mRNA expression studies indicated the potential benefit for wound closure. Histological evaluation of tissues with a pig model with incision and punch wounds showed that treatment with ONB-G exhibited improved healing compared with hydrogel without ONBs or treated without the gel. Our studies show that dextran-shell ONBs embedded in a gel (ONB-G) have the potential to accelerate wound healing, given its oxygen-holding capacity and release properties.

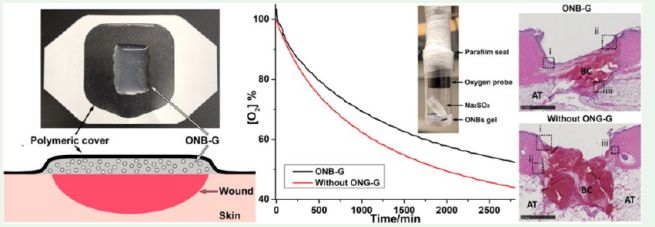

KEYWORDS: *oxygen encapsulation, nanobubbles, hydrogel, carbopol, wound healing*

INTRODUCTION

Acute or chronic wounds located on the largest organ, the skin, of humans often result in suffering and in the long term, significant morbidity to patients. While acute wounds are quite common in daily life, it is estimated that there are about 10 million people (2022 estimate) in the United States suffering from diabetic foot ulcers, one of the most common chronic wounds.[1,2] Development of treatment options for acute and chronic wounds and expedited recovery from surgical wounds can reduce patient suffering and improve surgical outcomes. It has been suggested that oxygen would accelerate the complex wound healing process, which encompasses multiple biological events such as cell proliferation and protein production.[3,4] To accelerate wound healing, one of the most common treatments recommended is oxygenation in a hyperbaric chamber where oxygen in the controlled environment can be adjusted to a set pressure and level for a fixed duration. However, hyperbaric chambers are not commonplace and easily accessible due to logistics, risk of exposure to high-pressure oxygen, and large size of the chambers, and they impose an unnecessary economic burden on the patient and system. Portable devices for oxygen delivery such as Topical Wound Oxygen (TWO2) therapy and OxyGeni exist but are potentially risky due to the risk of explosion from oxygen use/generation. Therefore, a need exists in the development of facile methods for oxygenation of wounds to accelerate healing.

Hydrogels are ideal materials for wound dressing and provide an optimal microenvironment for the wound.[5] Hydrogels have been utilized for anti-infection, adhesion and hemostasis, prevention of inflammation, and substance delivery.[6−8] Integrated with antibiotics or other compounds, hydrogels can prevent bacterial infection and deliver drugs to enhance wound care.[9−12] With a combination of antibiotics and drugs, multifunctional hydrogels have been reported for use as anti-infection agents and for neovascularization of chronic wounds.[13] Adhesive hydrogel could be used for sutureless wound closure.[14] Hydrogels can serve as a conducive matrix for oxygen delivery or generation at the wound surface to improve the healing process. Current products for oxygen provision to the wounds are generally grouped into the following categories: (i) hydrogel with dissolved oxygen or oxygen nanobubbles;[15,16] (ii) hydrogel where oxygen is generated from H_2O_2 or other substrates in a catalyzed reaction;[17−19] or (iii) hydrogel with bioactive species that would generate oxygen.[20−23]

Received: April 23, 2023
Accepted: June 30, 2023
Published: July 17, 2023

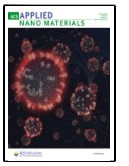

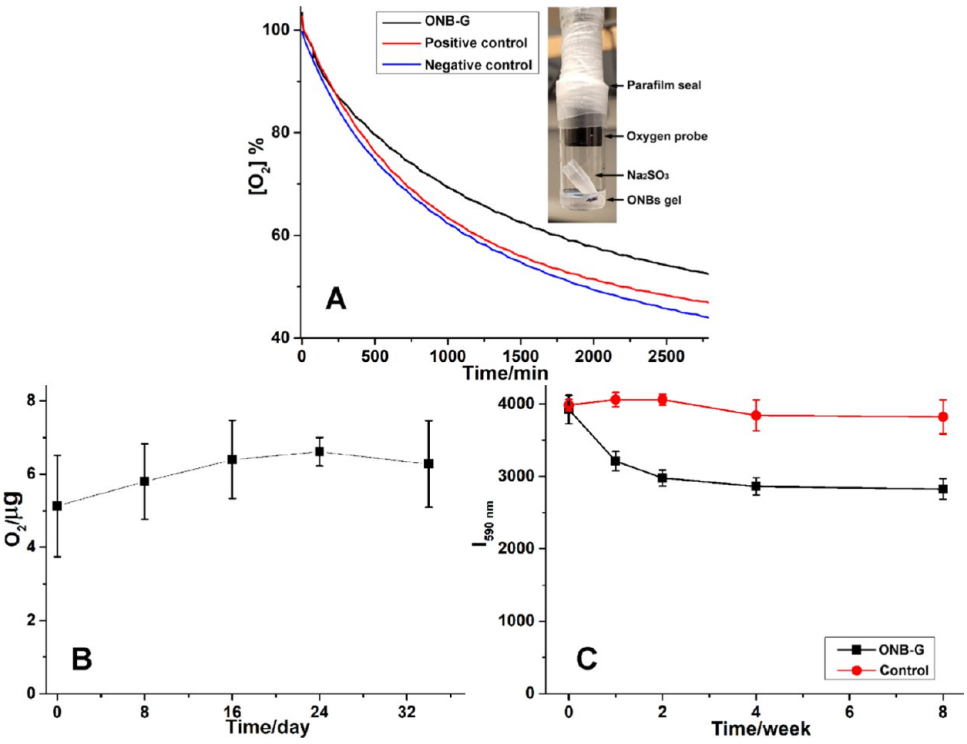

Figure 1. Oxygen concentration curve from ONB-G, hydrogel prepared with oxygen-saturated water as the positive control and without hydrogel as the negative control (A). Calculated oxygen release for 12 h from ONB-G stored at 4 °C (B). Fluorescence at 590 nm from $Ru(dpp)_3^{2+}$ in ONB-G and hydrogel without ONBs stored at serial times (C).

The amount of oxygen in the hydrogel based on dissolved oxygen is determined by the solubility of oxygen in the solvent. In some of the gel materials, chemicals such as perfluorocarbons have been used to improve the solubility of oxygen.[24] However, delivery of oxygen for a prolonged period of time is limited. Oxygen-generating reactions such as catalyzed H_2O_2 hydrolysis could provide sufficient oxygen in a hydrogel-based wound dressing. However, to guarantee that the reaction only occurs when the hydrogel is applied to the wounds, the substrates and catalysts should not interact prior to the application of the dressing to the wound. For the hydrogels containing catalysts such as MnO_2,[17] H_2O_2 needs to be stored separately and added in an incremental manner, making the application of the dressing more complex. For the hydrogels encapsulating H_2O_2, the hydrolysis of H_2O_2 prior to application and the potential reaction between H_2O_2 and the hydrogel component could influence the utility of hydrogel materials in healthcare. Oxygen-providing hydrogel has been produced by integrating the hydrogel and bioactive species such as microalgae or bacteria that could produce oxygen through photosynthesis.[21−23] However, the other products beyond oxygen generated during the bioactivity of these species also pose a concern due to the possible harm to patients' health, necessitating further investigation.

Oxygen nanobubbles (ONBs) are oxygen-encapsulating shells primarily based on materials such as polymers or lipids.[25−29] Compared with dissolved oxygen, ONBs could hold oxygen for an extended period of time when present in a suitable buffer.[30,31] In our own prior work, we have shown that ONBs can be used as ultrasound contrast agents[32,33] and in cancer therapy.[25,34,35] More recently, we have shown that ONBs could be used to treat central retinal artery occlusion, an ischemic condition of the retina.[36] Evaluation of ONBs and their characterization in several retinal cells also showed excellent promise of tissue preservation due to extended oxygenation.[31] We hypothesize that the integration of ONBs and the hydrogel would enable the development of new materials with excellent oxygen-holding capacity with extended-release characteristics to successfully treat oxygen deficit indications in acute as well as chronic wounds.

Herein, we report on the development of ONBs-embedded hydrogel (ONB-G) based on carbopol for wound healing applications. Carbopol is a polymer with high molecular weight and has been used in hydrogel preparation for drug delivery on patients' skin.[37−39] Furthermore, carbopol has been shown to have enhanced gelling properties (gels can be formed in 10 min), thus reducing the loss of oxygen during hydrogel preparation. The gel formation occurs at room temperature, making it a low-temperature process. The oxygen release and storage capability of the proposed ONB-G were first evaluated. We show that the hydrogel could continuously release oxygen for up to 46 h. Compared with the hydrogel prepared with oxygen-saturated water, ONB-G provides a significantly increased amount of oxygen. Meanwhile, the oxygen release capability of ONB-G remained at a similar level after 34 days of storage, exhibiting excellent oxygen-holding stability of the hydrogel. We further investigated the effect of carbopol concentration on oxygen release from the corresponding hydrogel. It can be noted that although the rheological properties of the hydrogel vary with the level of carbopol, the oxygen release features of these hydrogels are similar. We have also shown that ONB-G is sterile, i.e., it prevents bacterial growth and is nontoxic to adult human dermal fibroblasts (HDFa). Further experiments show that ONB-G can significantly increase wound closure in a scratch assay when applied to HDFa cells in hypoxia. mRNA expression studies

https://doi.org/10.1021/acsanm.3c01812
ACS Appl. Nano Mater. 2023, 6, 13116−13126

show that the ONB-G significantly reduced PAI-1, which is upregulated in hypoxia and contributes to impaired wound closure. *In vivo* acute wound studies in a pig model demonstrated significant closure of punch biopsy wounds and positively remodeled incision wounds as seen from histology staining. Compared with the wounds treated with hydrogel without ONBs or Tegaderm only, the histological results of the tissues from wounds treated with ONB-G exhibited improved healing benefiting from the oxygenated hydrogel dressing with ONBs. We expect that the current prototype of the ONB-G-based dressing could be further improved by minimizing oxygen loss during storage and at the application stage. Further effort is ongoing to develop better packages and dressing materials.

EXPERIMENTAL SECTION

Materials and Agents. Sodium sulfite, cobalt(II) chloride hexahydrate, D-(+)-trehalose dehydrate, potassium chloride, dextran sulfate sodium, D-α-tocopherol poly(ethylene glycol) 1000 succinate (TPGS), palmitic acid, and dextrose were purchased from Sigma-Aldrich (MO). Water used is Molecular Biology Grade water purchased from Mediatech. Inc. (VA). Tris(4,7-diphenyl-1,10-phenanthroline)ruthenium(II) ($Ru(dpp)_3^{2+}$) dichloride and sodium chloride were obtained from VWR International, LLC. Lecithin (DS-Soya PC80-C) is a gift from Solus Advanced Materials Co., Ltd. (Gyeonggi-do, S. Korea). Carbopol 940 was provided by Lubrizol Life Science (OH). Ethanol was obtained from Decon Labs Inc. (PA). Casein Peptone was purchased from Remel Products (Waltham, MA). Peptone S (Soy Peptone) was purchased from BioWorld (Dublin, OH). Dibasic potassium phosphate was purchased from Mallinckrodt Chemicals (Dublin, Ireland). All chemicals were used as received without further purification. Glassware for experiments was cleaned with the detergent and rinsed with DI water and autoclaved.

Preparation of ONBs. The preparation of ONBs was performed based on our previous work with minor changes.[31] Briefly, oxygen was blown into 10 mL of DI water at a pressure of 30 psi. The DI water was sonicated at 50 W with a 30 s sonication-on and 40 s sonication-off cycle. Under sonication, 0.2 mL of 0.045% potassium chloride aqua solution, 1 mL of 0.23% PC80 aqua solution, 0.4 mL of 0.028% TPGS aqua solution, 1 mL of 0.9% dextran aqua solution, 0.3 ml of 0.19% palmitic acid ethanol solution, and 0.4 mL of 0.4% trehalose aqua solution were added every two sonication cycles. The obtained solution was sonicated for four more cycles and filtered with a 0.22 μm filter. The filtered solution with ONBs was used to prepare ONB-G.

Preparation of ONB-G. Preparation of ONB-G was initiated by the addition of a calculated amount of Carbopol 940 directly into the ONBs solution. The obtained mixture was then strongly vortexed for 20 min at room temperature for complete dissolution of Carbopol 940. Gas bubbles generated during the vortex in the obtained mixture were eliminated by centrifugation at 8000 rpm for 30 s. Then, ONB-G without gas bubbles was thus fabricated. The hydrogel dressing obtained was stored at 4 °C in a sealed glass vial with an aluminum cap and rubber stopper for successive characterization.

Test of Oxygen Release. To investigate the oxygen release from the ONB-G, a test system was developed as illustrated in the inset of Figure 1A. An oxygen meter probe was sealed in a glass vial with a centrifuge tube containing 0.3 ml solution with 0.267 g/mL sodium sulfite and 99 μg/mL cobalt (II) chloride hexahydrate. Then, 1 mL of hydrogel sample was injected into the vial and then sealed again with parafilm. A Thermo Scientific Orion Versa Star Pro DO Benchtop Meter with optical dissolved oxygen probes (Ottawa, Ontario, Canada) was used to record the change in oxygen level in the vial at 1 min intervals.

Fluorescence Characterization. To investigate the change in the oxygen level in the hydrogel, $Ru(dpp)_3^{2+}$ was added to the Carbopol 940 and ONBs solution mixture before vortexing. The concentration of $Ru(dpp)_3^{2+}$ was adjusted to 66 μg/mL in the gel and fluorescence at 590 nm was recorded in 100 μL hydrogel sample volume in a 96-well plate with a BioTek Synergy HT plate reader.

Rheology Characterization. Rheological characterization was performed with an ARES-G2 oscillatory rheometer. ONB-G with 1, 1.5, and 2%(w/v) of Carbopol 940 was evaluated for rheological properties, while the hydrogel without ONBs was used as the control.

Bacterial Minimum Inhibitory Content. Soybean-Casein media was made following the U.S. Pharmacopeia Sterility ⟨71⟩ recipe and cited elsewhere.[31] Briefly, 1.7 w/v % Casein Peptone, 0.3 w/v% Peptone S (Soy Peptone), 0.5 w/v% sodium chloride 0.5, 0.25 w/v% dibasic potassium phosphate 0.25, and 0.23 w/v% dextrose were dissolved in 1 L of purified water. The pH was adjusted to 7.3 ± 0.2 using 1 M NaOH and sterilized using an autoclave.

Hydrogels were prepared via an aseptic technique as described above the day before experiments. The following day, 0.1, 0.5, or 1.0 g (n = 3) of hydrogel was placed in separate round bottom tubes and fresh soybean−casein media was added to reach a volume of 3 mL. *Staphylococcus aureas* at 0.5 × 10^8 CFU/mL was evaluated as a positive control, and media only (no inoculation) was used as the negative control. The samples were inoculated with *S. aureas* at 0.5 × 10^8 CFU/mL unless otherwise specified, incubated for 48 h at 37 °C, and agitated at 300 RPM. The optical density was read using an Eppendorf's BioPhotometer with 1 mL of each sample and a 1× PBS solution was used as blank.

Evaluation of Hydrogel Sterility. Soybean-Casein media was prepared as above, and the sterility test conducted followed the US Pharmacopeia Sterility ⟨71⟩ guidelines. Hydrogel samples were made the day before and added to sterile 50 mL tubes at n = 3. Media was used as a negative control. For positive controls, media was inoculated with the following: *Bacillus subtilis*, *S. aureus*, *Pseudomonas aeruginosa* 14 (PA14), and *P. aeruginosa* 01 (PA01). The samples were incubated at room temperature for 14 days. The optical density was read each day with 1 mL of the sample in a clean cuvette with 1× PBS as a blank. The sample was returned to the respective 50 mL tubes and incubated at room temperature.

Cell Culture. Primary Human Dermal Fibroblast (HDFa, PCS-201-012, ATCC) cells were cultured in Fibroblast Basal Medium (PCS-201-013, ATCC) supplemented with the Fibroblast Growth Kit-Low Serum (PCS-201-041, ATCC), 1× Antimycotic−Antibiotic (15240096, Thermo Fisher) at 37 °C, 5% CO_2.

Cell Viability. *Normoxic Conditions.* Cells were seeded at 5000 cells/well in 96-well plates and incubated overnight with eight replicates. The next day, fresh media was exchanged and the cells were treated with either 2 or 5 mg of ONB-G, or 2 or 5 mg of hydrogel without ONBs for 24 h. The following day, MTT assay was performed to evaluate cell viability.

Hypoxic Conditions. HDFa cells were seeded in a similar manner as above in 96-well plates. After overnight attachment, the media was removed and replaced with fresh media and the cells were then treated with either 2 or 5 mg of ONB-G and placed in a humidified hypoxic chamber with 3% O_2, 5% CO_2, and 92% N_2 at 37 °C for 24 h. The next day, the media was exchanged for fresh media and MTT assay was performed.

Scratch Assay. The day before the experiment, cells were seeded at 5 × 10^4 cells/well in Ibidi culture two well inserts (80209, Gräfelfing, Germany) with n = 2 and cultured overnight to ensure cell attachment. The next morning, the cell culture inserts were removed and images were taken at 4× magnification in bright field. The cells were then treated with either ONB-G at 2 or 5 mg, or hydrogel alone at 2 or 5 mg and placed in a humidified hypoxic chamber (3% O_2, 5% CO_2, and 92% N_2) at 37 °C for 24 h. The following day, the media was replaced with fresh media, and images were taken again at 4× magnification. For quantitative analysis, four images per well of different areas of the scratch assay were taken. ImageJ was utilized to measure the distance between the two sides of the scratch at the initial and final time points. The percent of scratch closure was determined per the equation

$$\text{scratch closure} = \frac{\text{initial distance} - \text{final distance}}{\text{initial distance}}$$

https://doi.org/10.1021/acsanm.3c01812
ACS Appl. Nano Mater. 2023, 6, 13116−13126

Hypoxic Gene Expression. The day before the experiment, cells were seeded at 0.6×10^6 cells/well at $n = 2$ in a 6-well plate. The following day, the cells were given fresh media and treated with 2 or 5 mg of the ONB-G or no treatment. The cells were placed in a humidified hypoxic chamber for 6 h in the same manner as before. Cells were then washed with 1× PBS, trypsinized, pelleted, and washed again with 1× PBS. The total RNA was extracted with Thermo Fisher's RNA Purification kit (K0731, Waltham, MA) following manufacturer's instructions. cDNA was synthesized with Applied Biosystem's High-Capacity cDNA Reverse Transcription kit (4368814, Waltham, MA) following manufacturer's instructions. With the primers shown in Table 1, RT-PCR analysis was conducted using

Table 1. Primers for Target Amplification

primer	forward	reverse
HIF-1α	CTG AGA GGT TGA GGG ACG GA	GGA AGT GGC AAC TGA TGA GC
PAI-1	GCA AGG CAC CTC TGA GAA CT	GGG TGA GAA AAC CAC GTT GC
VEGF-A	CGA AAG CGC AAG AAA TCC CG	GCT CCA GGG CAT TAG ACA GC

Applied Biosystem's PowerUp SYBR Green Master Mix (A25742, Waltham, MA) for PCR following manufacturer's instructions with n = 3 and 2 ng of cDNA per well.

Animal husbandry and Wound Treatment. *In vivo* experiments with a pig model were conducted per the protocol (IACUC Protocol#: 22133) approved by the University of Illinois Urabana-Champaign. An intramuscular injection of ceftiofur (5 mg/kg) was given to the animal 5−7 days before surgery. Additionally, the animal was made to fast for 12 h before the surgery. On the day of surgery, an intramuscular anesthetic of a telazol−atropine−rompun−ketamine cocktail was administered, and the surgical area was shaved and cleaned.

A sterile 8 mm biopsy punch was utilized to create identical wounds for $n = 3$ per treatment with a 1 cm spacing. The wound was then pressure held with gauze to stop excessive bleeding. Next, 3 incisions ∼2 cm long were made through the dermis and fascia. The incisions were closed with nondissolvable silk sutures.

The wounds were treated with ONB-G or hydrogel without ONBs and covered with a 6 cm × 6 cm PVC sheet to prevent oxygen release away from the wound. Wounds with no treatment were used as a negative control. All wounds were covered with Nexcare's Tegaderm transparent dressing (H1626, St. Paul, MN). Benamine S was given intramuscularly at 2.3 mg/kg prior to surgery and prophylactically every 12 h. On day 3 after surgery, the animal was sacrificed, tissues excised, and fixed in 4% neutral buffered saline.

Statistical Analysis. Statistical analysis was conducted with the R Studio statistical software. For MTT analysis, eight replicas were evaluated. Bacterial minimum inhibitory concentration, RT-PCR, sterility, and wound analysis were evaluated with three replicates. The scratch assay had two replicates, with four measurements taken per image. A one-way ANOVA followed by a post hoc Tukey test was used to determine the statistical difference between groups. Results were considered significant if the resulting p-value was less than 0.05.

RESULTS AND DISCUSSION

Scheme 1 illustrates the preparation and major composition of the proposed ONB-G. The ONBs were first synthesized as described in the Experimental Section and were dispersed in water and sealed in a closed container. Then, ONB-G was prepared without heating or prolonging the procedure by dissolving Carbopol 940 in the ONBs solution. The gelling procedure could be achieved in a sealed container in 20 min, minimizing the possible loss of oxygen from the ONB-G. Utilizing the carbopol hydrogel as the matrix, as-prepared ONBs were dispersed to store oxygen and release at the

Scheme 1. Schematic of ONB-G with a Polymeric Cover (Provided with Tegaderm) for Wound Dressing

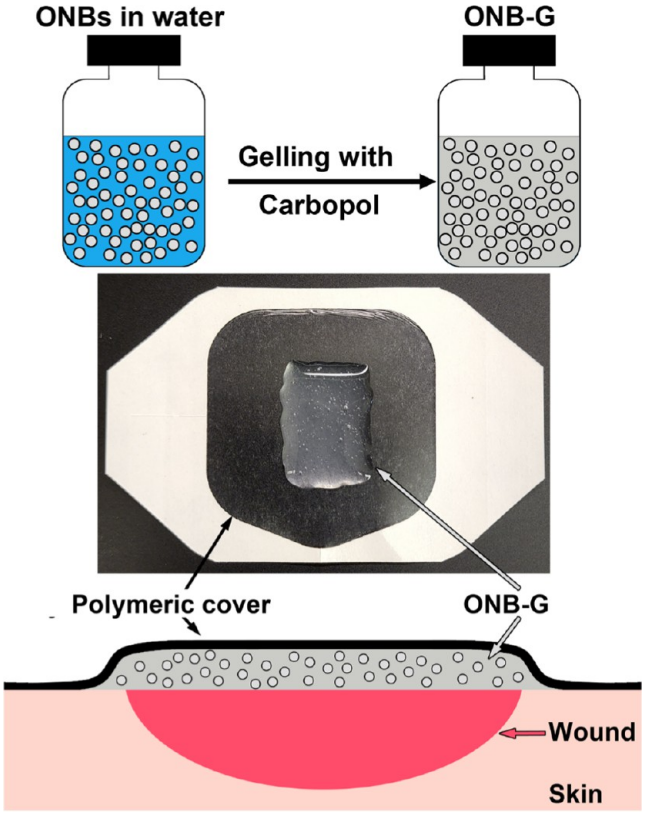

application site, for oxygenation around the wound. ONB-G could be sealed in a container then applied on the wound and covered with an oxygen-tight dressing upon application. Another possible way is to preload ONB-G in an oxygen-tight dressing and sealed in a package that can then be removed and the ONB-G applied along with the dressing to the wound as shown in Scheme 1. A polymeric cover was provided by Tegaderm in our application, which was used to fix the ONB-G hydrogel to the wound. The cover would also reduce the oxygen loss from the ONB-G to the environment.

To investigate oxygen release from ONB-G, experiments were conducted per the experimental setup shown as an inset in Figure 1A. The solution with sodium sulfite and cobalt (II) chloride in the centrifuge tube would continuously consume oxygen in the sealed test system. The change in oxygen level in the test system due to oxygen consumption is depicted as the negative control in Figure 1A. An oxygen concentration curve shows a consistent decrease in oxygen as demonstrated by the consumption of oxygen in the system with sodium sulfite. When the positive control of the hydrogel prepared with oxygen-saturated water was injected into the test system, a slightly higher level of oxygen was observed compared with the negative control. It is proposed that the increase in the oxygen level could be due to the oxygen-saturated water utilized as the positive control. When the ONB-G was injected into the test system, an oxygen concentration curve with a much higher oxygen level was obtained. It can be noted from the test system that the ONB-G sustained a higher oxygen level than the positive control hydrogel and negative control hydrogel. The difference in the oxygen level confirmed that the ONB-G has the capacity to deliver oxygen due to the embedded ONBs.

https://doi.org/10.1021/acsanm.3c01812
ACS Appl. Nano Mater. 2023, 6, 13116−13126

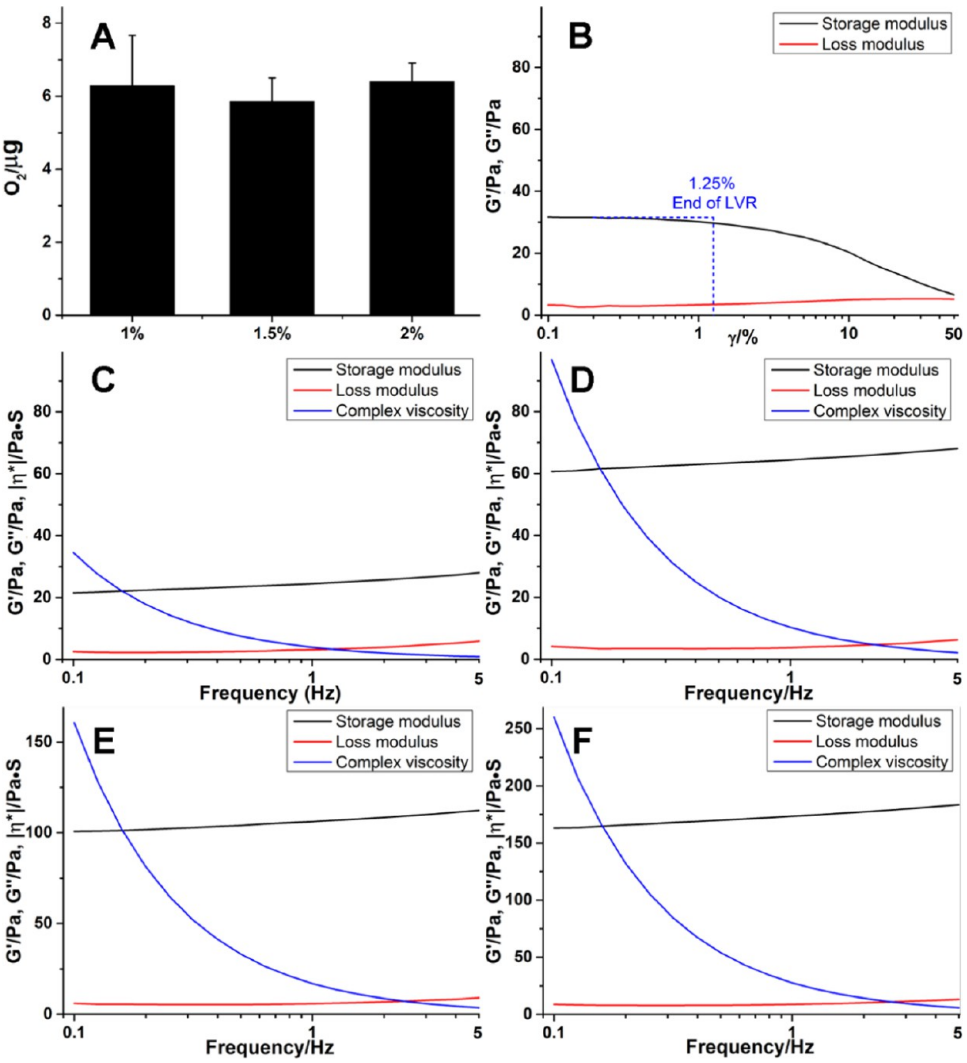

Figure 2. Oxygen release from ONB-G prepared with various concentrations of Carbopol 940 (A). Rheology characterization of ONB-G by amplitude sweep (B) and frequency sweep (C). Frequency test of hydrogel without ONBs (D) as control. Frequency sweep characterization of ONB-containing gel prepared with 1.5% (E) and 2% (F) Carbopol 940.

Based on the difference in oxygen concentration curves from ONB-G and the negative control, a calculation was performed to evaluate the amount of oxygen released from ONB-G in 12 h

$$w_{\text{oxygen}} = (C_{0\text{h NC}} - C_{12\text{h NC}}) \times V - (C_{0\text{h ONBs}} - C_{12\text{h ONBs}}) \times (V - 1)$$

where w_{oxygen} is the weight of oxygen released from the ONB-G hydrogel, $C_{0\text{h NC}}$ and $C_{12\text{h NC}}$ are the oxygen concentration initially and after 12 h in relation to the negative control, $C_{0\text{h ONBs}}$ and $C_{12\text{h ONBs}}$ denote the initial and 12-h oxygen concentration in the ONB-G, and V is the volume of the space in the test setup. The calculation provides an approximate indication of the amount of oxygen from ONB-G. Figure 1B shows the oxygen released in 12 h from ONB-G upon storage. A slight increase was noted in the average amount of oxygen released from freshly prepared ONB-G compared to the stored ONB-G hydrogel, which could be attributed to the aging of the carbopol-based hydrogel.[40] There was no observable decrease in the oxygen release capacity of ONB-G noted over the 34-day storage period. A picture of fresh ONB-G and ONB-G stored for different periods is provided in Figure S1. It can be seen that there is no significant difference in the hydrogel status of the ONB-G over the storage.

To further confirm the oxygen storage capability of the ONB-G hydrogel, $Ru(dpp)_3^{2+}$, a fluorophore sensitive to oxygen was used to track the change in oxygen level in the ONB-G. It is known that the fluorescence from $Ru(dpp)_3^{2+}$ will decrease in the presence of oxygen, making it suitable for monitoring oxygen in the hydrogel.[41,42] The fluorescence intensity at 590 nm was used to evaluate the change in fluorescence of $Ru(dpp)_3^{2+}$ in the hydrogel and the results are shown in Figure 1C. It can be seen that there is a distinct decrease in the fluorescence intensity from the ONB-G after 1 week; in contrast, the fluorescence intensity in the control, hydrogel without ONBs, showed no significant change. The difference between the ONB-G and hydrogel without ONBs indicated the oxygen release from the ONBs embedded in the hydrogel. Furthermore, it can be noted that the decrease in the fluorescence from $Ru(dpp)_3^{2+}$ continued until Week 4, indicating that after 4 weeks the oxygen level in the test system is high enough to induce an observable decrease in the fluorescence intensity. The results shown in Figure 1C

https://doi.org/10.1021/acsanm.3c01812
ACS Appl. Nano Mater. 2023, 6, 13116−13126

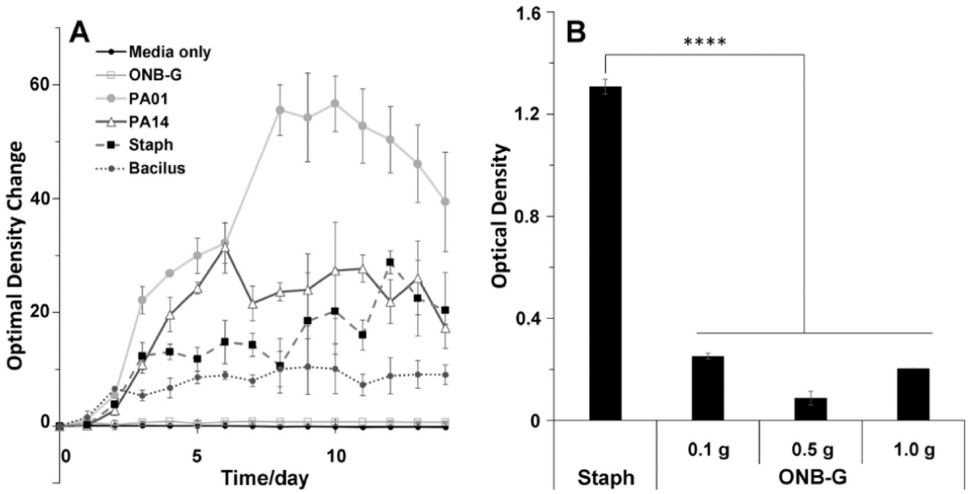

Figure 3. Sterility assessment of hydrogels. Sterility experiments follow U.S. Pharmacopoeia Sterility ⟨71⟩ protocol (A). Minimum inhibitory concentration against *S. aureas* and various amounts of ONB-G (B).

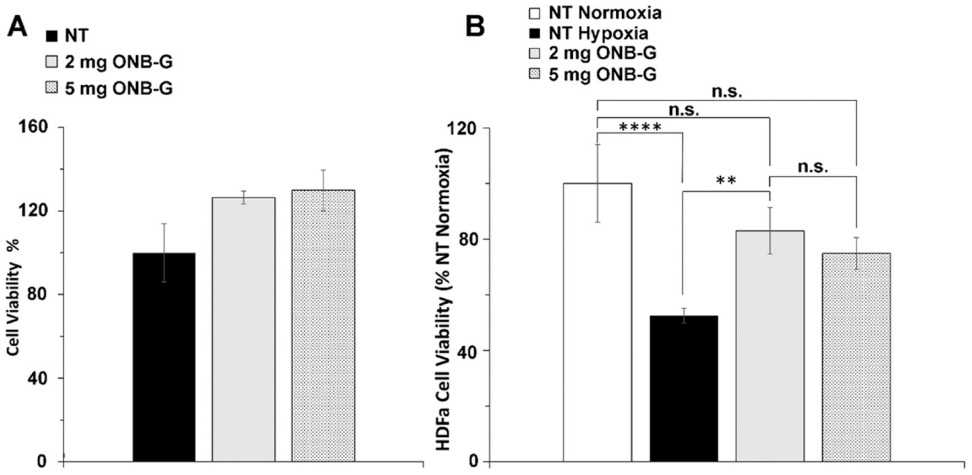

Figure 4. HDFa cell viability studies. HDFa cells cultured in normoxic conditions and treated with ONB-G at 2 mg or 5 mg concentration (A). HDFa cell viability in hypoxia treated with either 2 or 5 mg of ONB-G (B). Data shown as mean ± standard deviation. $n = 8$. "n.s." indicates no significant difference between groups. $^{**}p < 0.01$, **** $p < 0.0001$.

demonstrate the potential of ONB-G to retain a high level of oxygen for a prolonged period of time.

The effect of carbopol concentration in the hydrogel on the oxygen release capability was also evaluated. ONB-G was prepared with carbopol at 1, 1.5, and 2%. The oxygen released from the ONB-G was tested and the results are shown in Figure 2A. The release profiles show that the oxygen content released from these ONB-G are similar, indicating that the effect of carbopol concentration on the oxygen release property in the hydrogel is minimal.

The rheological properties of the ONB-G gel were characterized and the results are shown in Figure 2B–F. The amplitude sweep test at a frequency of 1 Hz (Figure 2B) indicated that the linear viscoelastic region of the ONB-G hydrogel is below a strain level of 1.25%. Meanwhile, at a strain level of less than 50%, the storage modulus (G') is always higher than the loss modulus (G''), indicating a solid-like viscoelastic property of the ONB-G. Figure 2C shows the results from frequency sweep tests with ONB-G evaluated at a strain level of 1%. A larger G' than G'' in the range from 0.1 to 5 Hz can be noted, highlighting the dominant elastic property of the ONB-G gel. The complex viscosity ($|\eta^*|$) decreased with an increase in frequency, indicating a shear-thinning characteristic of the ONB-G. The hydrogel without ONBs was also tested and its frequency sweep results are shown in Figure 2D. A significant difference in storage modulus, loss modulus, and complex viscosity between ONB-G gel and hydrogel without ONBs indicated that the presence of ONBs in the hydrogel would influence the viscoelastic behavior of the hydrogel. Meanwhile, as in Figure 2E,F, test results from hydrogels fabricated with 1.5 and 2% Carbopol 940 showed that the rheological properties of the hydrogel depend on the concentration of Carbopol 940 in the ONB-G product.

It is essential that the ONB-G hydrogel is sterile and does not favor bacterial growth. The sterility of the hydrogel was evaluated following the U.S. Pharmacopeoia ⟨71⟩ Sterility protocol.[43] From Figure 3A, the optical density of the ONB-G hydrogel and media-only samples did not increase from the baseline for 14 days, indicating the absence of bacterial growth. In contrast, samples of *B. subtilis*, *S. aureus*, *P. aeruginosa* 14 (PA14), and *P. aeruginosa* 01 (PA01) exhibited a sharp increase in optical density after 48 h. Additionally, minimum inhibitory concentration was tested against *S. aureus* with varying amount of the hydrogel. As shown in Figure 3B, the

https://doi.org/10.1021/acsanm.3c01812
ACS Appl. Nano Mater. 2023, 6, 13116−13126

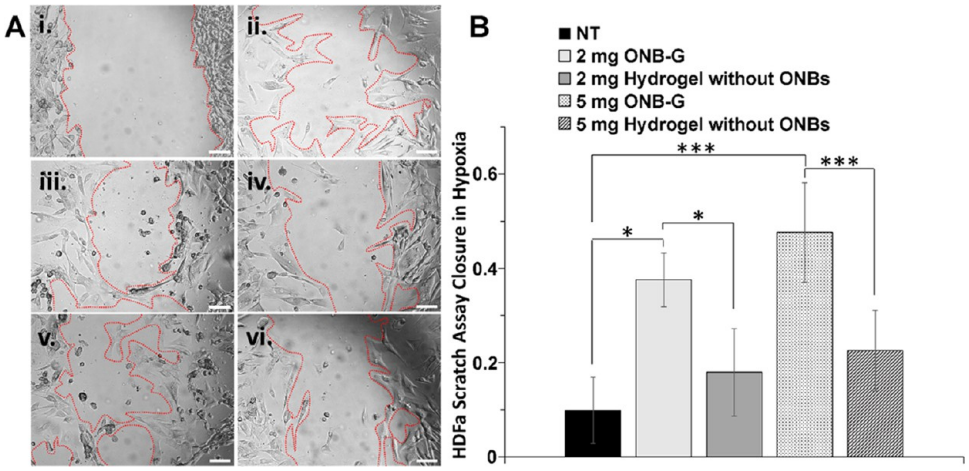

Figure 5. HDFa scratch assay. HDFa cells cultured in hypoxic conditions before treatment (i) and after incubation in hypoxia with no treatment (ii), 2 mg ONB-G (iii), 2 mg hydrogel without ONBs (iv), 5 mg ONB-G (v), or 5 mg hydrogel without ONBs (vi). The red dashed line indicates HDFa cell borders (A, scale bar = 100 μm). HDFa cell viability in hypoxia treated with either 2 or 5 mg ONB-G, or 2 or 5 mg of hydrogels without ONBs (B). Data shown as mean ± standard deviation. $n = 4$. *$p < 0.05$, ***$p < 0.001$.

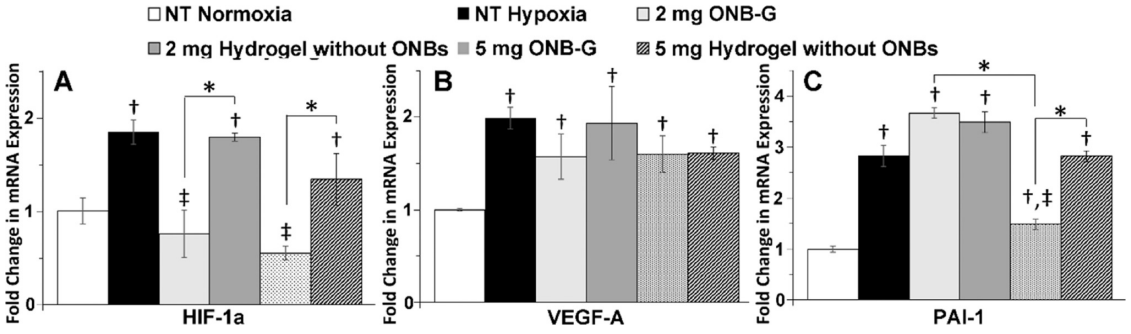

Figure 6. RT-PCR analysis of hypoxic genes. HDFa cells were cultured in either normoxic or hypoxic (3% O_2) conditions for 6 h. Evaluation of mRNA expression of HIF-1α. The ONB-G has a significant effect on the HIF-1α expression at both the 2 and 5 mg dose levels (A). Evaluation of mRNA expression of VEGF-A (B). Evaluation of mRNA expression of PAI-1 (C). †Significantly different from the NT Normoxia group. ‡Significantly different from the NT Hypoxia group. *$p < 0.05$.

hydrogel amount of 0.1, 0.5, and 1.0 g exhibited significantly lower bacterial growth after 24 h of incubation, indicating that the hydrogel is synthesized aseptically and can inhibit bacterial growth.

Another essential requirement is that the hydrogel does not damage the dermis. Therefore, viability tests with HDFa skin cells were evaluated. The skin cells were treated with 2 or 5 mg of hydrogel, and at normoxia (20% O_2) and no cell death was noted as indicated by ~100% viability in each tested group. In hypoxia (3% O_2), with the untreated cells under normoxic conditions as the reference with 100% viability, the untreated cells had a viability of 56.6 ± 7.03% compared to the 2 mg dose that had 85.5 ± 8.31% and the 5 mg dose had 74.9 ± 5.72% viability (Figure 4). The presence of the ONB-G hydrogels significantly increased cell viability when cultured in a hypoxic environment. Additionally, there was no significant difference between either 2 mg or 5 mg ONB-G hydrogels in hypoxia compared to that of HDFa cells cultured in normoxic conditions. Therefore, the ONB-G hydrogel promoted a conducive environment for HDFa cell growth that is similar to that under normoxic conditions. Here, the ONB-G hydrogel did not cause cell death but promoted cell survival in hypoxic environments.

To test the efficacy of the ONB-G hydrogel, a scratch assay was performed in a hypoxic environment. After 24 h of incubation in hypoxia with either 2 or 5 mg of ONB-G, 2 or 5 mg of hydrogel without ONBs, or no treatment, there is a significant difference between treated and untreated cells. Compared to the initial scratch distance shown in Figure 5A(i), the ONB-G hydrogels (Figure 5A(iii,v)) had substantial growth to close the simulated wound. The hydrogel without ONBs (Figure 5A(iv,vi)) did not provide an adequate environment for wound closure. However, increased wound closure was noted in the hydrogels without ONBs than in the no-treatment group. This could indicate that properties intrinsic to the carbopol hydrogel can promote cell growth and wound closure.

To quantify the scratch assay, the distance between the wound edges was measured via the NIH ImageJ software. Figure 5B shows that both the 2 and 5 mg ONB-G hydrogels had significantly more scratch closure than the no-treatment group. Additionally, the presence of ONBs had a significant effect on wound closure. The hydrogel without ONBs at both doses had more scratch closure than the no-treatment group, but it was not significant, indicating that Carbopol 940 has innate properties that could promote wound healing. Our results are consistent with migration studies of primary cells from skin biopsies.[44] Under hypoxic conditions, keratinocytes had significantly less migration than those cultured under

https://doi.org/10.1021/acsanm.3c01812
ACS Appl. Nano Mater. 2023, 6, 13116−13126

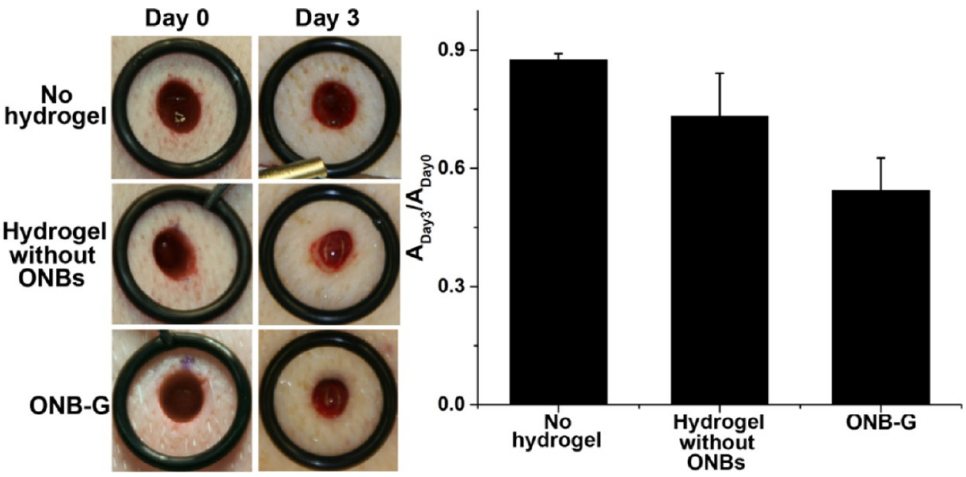

Figure 7. Image of wounds on Day 0 and Day 3 after treatment with no hydrogel, hydrogel without ONBs, and ONB-G along with the corresponding wound area ratio.

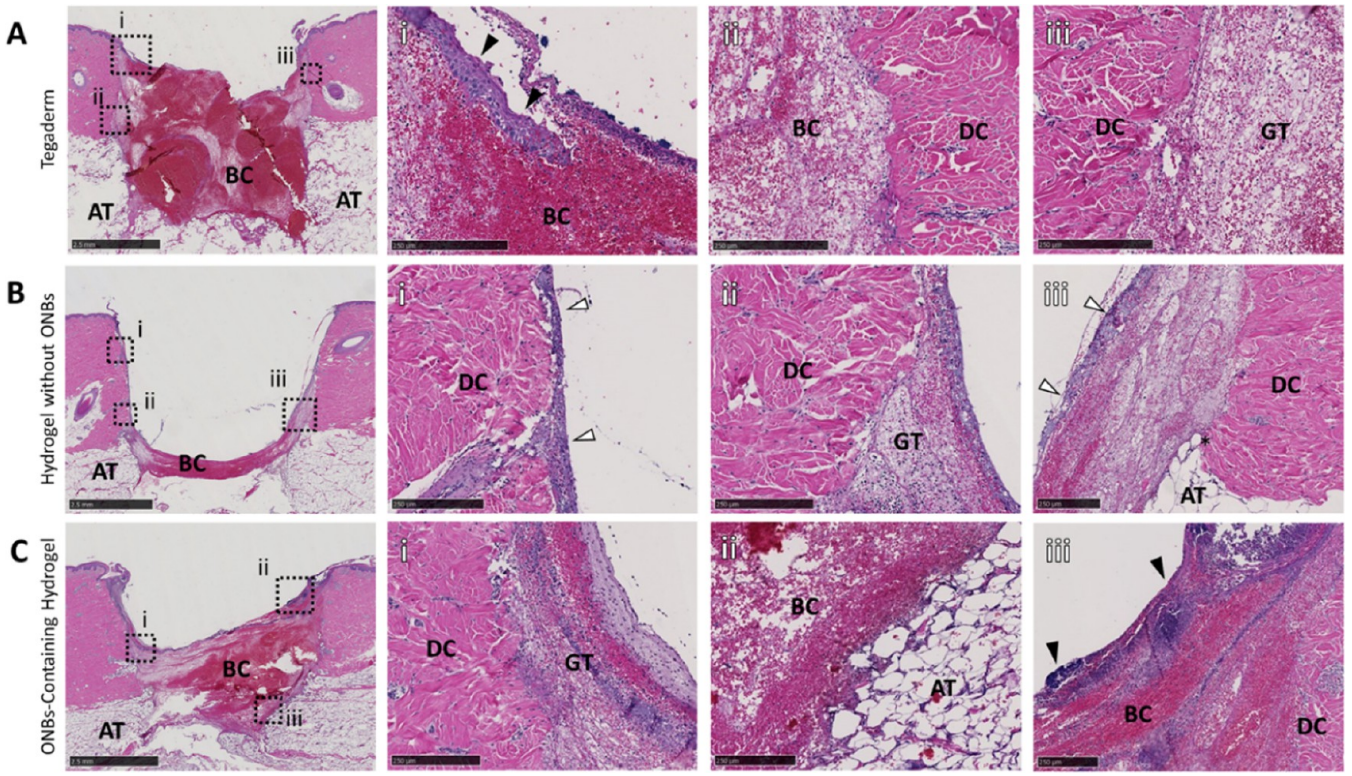

Figure 8. Histological sections of 8 mm punch wounds stained with H&E on Day 3 after treatment. Sections include punch wounds treated with Tegaderm (A), hydrogel without ONBs (B), or ONB-G (C). The dotted boxes in column 1 correspond to the magnified images in columns 2, 3, and 4. Closed arrows indicate reepithelialization. Open arrows indicate immature epithelialization. Other highlighted sections are the blood clot (BC), adipose tissue (AT), granulation tissue (GT), and dermal collagen (DC). The scale bar in the original image is 2.5 mm. Scale bar in the magnified image is 250 μm.

normoxic conditions. With ONB-G, the cells were able to increase their cell migration properties even in hypoxia.

Under hypoxic conditions, various genes were affected. Genes that are upregulated in hypoxic or wounded environments are HIF-1α, VEGF-a, and PAI-1. It has been shown that HIF-1α and VEGF-a are upregulated in response to hypoxia to promote vasculogenesis, erythropoiesis, and other pathways to increase oxygen delivery to the hypoxic area.[45−47] PAI-1 is upregulated in hypoxia due to an enzyme known to inhibit the cleavage plasminogen to form plasmin, which results in the inhibition of fibrinolysis in wounds and blood clots.[48] In our study, we found that HIF-1α and PAI-1 were expressed at a significantly lower rate compared to the NT Normoxia group. Both the 2 mg and 5 mg ONB-G hydrogels provided sufficient oxygen to lower the HIF-1α levels significantly from the NT hypoxia group. Additionally, it is shown that the ONBs present in the hydrogel contribute to the downregulation of HIF-1α (Figure 6A). Additionally, the 5 mg ONB-G hydrogel significantly lowered the expression of PAI-1 mRNA compared to the NT hypoxia group, but the 2 mg ONB-G hydrogel did not have this effect (Figure 6C). The additional oxygen stored in the 5 mg ONB-G hydrogel allowed the cells to lower the

https://doi.org/10.1021/acsanm.3c01812
ACS Appl. Nano Mater. 2023, 6, 13116−13126

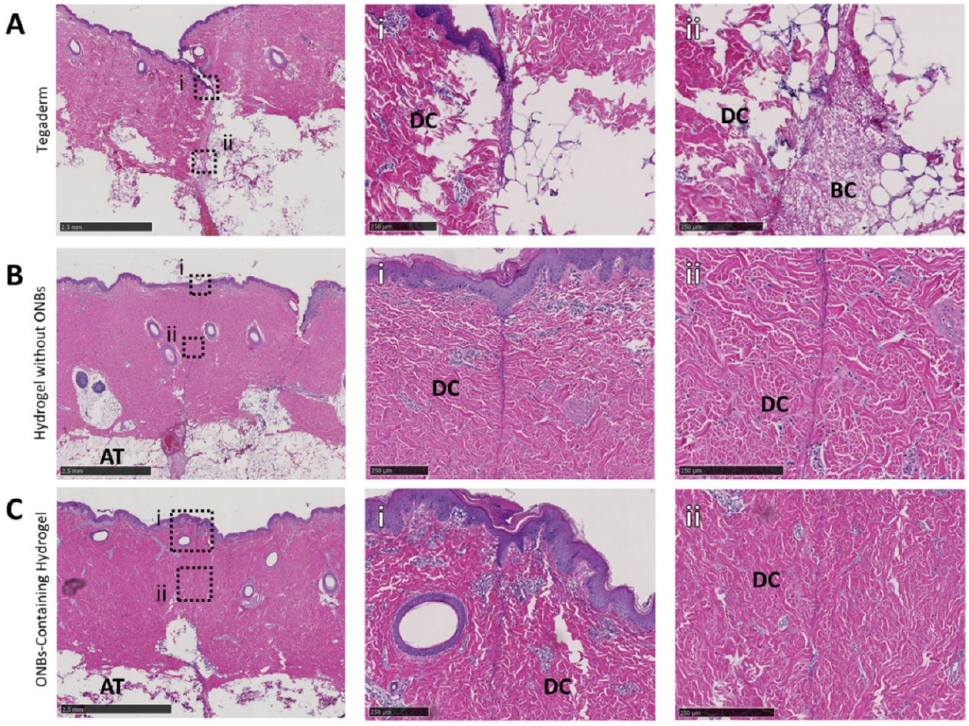

Figure 9. Histological sections of incision wounds stained with H&E on Day 3 after treatment. Sections include incisions treated with Tegaderm (A), hydrogel without ONBs (B), or ONB-G (C). The magnified images of the dotted boxes in column 1 are provided in columns 2 and 3. Highlighted areas include dermal collagen (DC), adipose tissue (AT), and blood clot (BC). The scale bar in the original image is 2.5 mm. Scale bar in the magnified images is 250 μm.

PAI-1 expression, but it was still significantly higher than the cells in the NT Normoxia group. Lastly, VEGF-A was not significantly altered in hypoxia after treatment with the hydrogels. There is a slight decrease in VEGF-A expression in the 2 mg ONB-G compared to the 2 mg hydrogel without ONBs, but it was not significant (Figure 6B).

The porcine *in vivo* model was treated with both the ONB-G and the hydrogel without ONBs. Tegaderm, which is a commercially available wound dressing film, was used as a negative control. After 3 days of treatment, tissues from punch and incision wounds were collected and processed. Figure 7 shows images of typical punch wounds on Day 0 and Day 3. It can be seen that there is no significant change in the morphology of the wound treated without hydrogel. When the wound was treated with hydrogel without ONBs, a decrease in wound size could be seen, but the edge of the wound on Day 3 is similar to that on Day 0. The wound treated with ONB-G shows a shrinkage of the wound area, while the edge of the wound exhibited observable morphology change, suggesting a better healing. Comparison of the change in the morphology of wounds with different treatments indicates that the ONB-G could significantly enhance healing of the wound. Histological sections showed that after 3 days of healing, varying amounts of granulation tissue were present underneath the blood clot. As shown in Figure 8, the punch wound treated with ONB-G hydrogel (Figure 8A) had a lower wound depth excluding the blood clot compared to the Tegaderm and hydrogel without ONBs (Figure 8B,C). However, the wound treated with ONB-G hydrogel shows signs of reepithelialization across the wound bed, shown as filled in arrows (Figure 8C(iii)). Although the Tegaderm and hydrogel without ONBs show reepithelialization, it is either immature (Figure 8B(i)) or did not span the entire wound bed (Figure 8A(i)). In the incision wound, the Tegaderm-treated incision did not close to the top of the wound (Figure 9A(i)); in contrast, a clear closure can be observed on the top of the wounds treated with hydrogel without ONBs (Figure 9B(i)) or ONB-G (Figure 9C(i)). Further, in the hydrogel without ONBs, there is blood in the incision wound, whereas in the incision wound treated with ONB-G, there is no blood and the wound fused more clearly. The difference between the wounds treated with carbopol-based hydrogel, containing ONBs or without, and with Tegaderm demonstrated that the dressing with carbopol-based hydrogel would be beneficial to the wound healing process. Furthermore, it should be noted that the wounds treated with ONB-G healed even faster, especially at the deeper sections of the wound, than the wounds treated with hydrogel without ONBs, affirming that the oxygen delivered by the ONBs in the hydrogel accelerates the healing process.

■ CONCLUSIONS

Herein, we propose oxygen nanobubbles-embedded carbopol-based hydrogel as a wound dressing material that could hold and deliver oxygen to the wound bed to accelerate healing. We show that ONB-G has the ability to slowly release oxygen to relieve wounds of hypoxia to maintain normoxic conditions. Extending our stability studies with ONBs, storage studies indicated that the proposed ONB-G could store oxygen for up to 34 days. It is noted that an increase in carbopol concentration in the ONB-G did not influence oxygen release capacity of the hydrogel, though the rheological properties of the ONB-G were altered with carbopol concentration. Sterility tests show that the fabricated ONB-G was sterile and HDFa cell-based investigations with ONB-G exhibited excellent potential in reviving cells in hypoxia. Experiments in a pig model with incision and punch wounds validated the wound

https://doi.org/10.1021/acsanm.3c01812
ACS Appl. Nano Mater. 2023, 6, 13116−13126

healing characteristics of ONB-G. Histological studies confirm that the carbopol-based hydrogel with embedded ONBs could significantly accelerate wound healing as demonstrated in our acute wound studies. The proposed approach shows promise and could be further developed to treat acute surgical as well as chronic wounds. The demonstrated approach is less expensive and could serve as an alternative for the hyperbaric oxygen chamber.

■ ASSOCIATED CONTENT

Supporting Information

The Supporting Information is available free of charge at https://pubs.acs.org/doi/10.1021/acsanm.3c01812.

Fresh ONB-G and the ONB-G stored for 1 week, 2 weeks and 5 weeks (PDF)

■ AUTHOR INFORMATION

Corresponding Author

Joseph Irudayaraj − *Department of Bioengineering, Beckman Institute, Carl Woese Institute of Genomic Biology, & Micro and Nanotechnology Laboratory, and Cancer Center at Illinois (CCIL), University of Illinois at Urbana-Champaign, Urbana, Illinois 61801, United States; Biomedical Research Center in Mills Breast Cancer Institute, Carle Foundation Hospital, Champaign, Illinois 61801, United States; Carle-Illinois College of Medicine, Urbana, Illinois 61801, United States;* orcid.org/0000-0002-0630-1520; Email: jirudaya@illinois.edu

Authors

Wen Ren − *Department of Bioengineering, University of Illinois at Urbana-Champaign, Urbana, Illinois 61801, United States; Biomedical Research Center in Mills Breast Cancer Institute, Carle Foundation Hospital, Champaign, Illinois 61801, United States*

Victoria Messerschmidt − *Biomedical Research Center in Mills Breast Cancer Institute, Carle Foundation Hospital, Champaign, Illinois 61801, United States; Revive Biotechnology, Inc., Champaign, Illinois 618 20, United States*

Michael Tsipursky − *Vitreo-Retinal Surgery, Ophthalmology Department, Carle Foundation Hospital, Urbana, Illinois 61801, United States; Carle-Illinois College of Medicine, Urbana, Illinois 61801, United States; Revive Biotechnology, Inc., Champaign, Illinois 618 20, United States*

Complete contact information is available at: https://pubs.acs.org/10.1021/acsanm.3c01812

Notes

The authors declare the following competing financial interest(s): We have applyied for a Patent and potentially have a company license our technology.

■ ACKNOWLEDGMENTS

The authors acknowledge partial seed funding from the Health Maker Lab (HML) of the Carle-Illinois College of Medicine and support from NSF Award# 2031313.

■ REFERENCES

(1) Centers of Disease Control and Prevention, National Diabetes Statistics Report 2022 https://www.cdc.gov/diabetes/data/statistics-report/index.html?ACSTrackingID=DM72996&ACSTrackingLabel=New%20Report%20Shares%20Latest%20Diabetes%20Stats%20&deliveryName=DM72996 (accessed 2022-06-29).

(2) Singh, N.; Armstrong, D. G.; Lipsky, B. A. Preventing foot ulcers in patients with diabetes. *JAMA* **2005**, *293*, 217−228.

(3) Castilla, D. M.; Liu, Z. J.; Velazquez, O. C. Oxygen: Implications for Wound Healing. *Adv. Wound Care* **2012**, *1*, 225−230.

(4) de Smet, G. H.; Kroese, L. F.; Menon, A. G.; Jeekel, J.; van Pelt, A. W.; Kleinrensink, G. J.; Lange, J. F. Oxygen therapies and their effects on wound healing. *Wound Repair Regen.* **2017**, *25*, 591−608.

(5) Fan, F.; Saha, S.; Hanjaya-Putra, D. Biomimetic hydrogels to promote wound healing. *Front. Bioeng. Biotechnol.* **2021**, *9*, No. 718377.

(6) Liang, Y.; He, J.; Guo, B. Functional hydrogels as wound dressing to enhance wound healing. *ACS Nano* **2021**, *15*, 12687−12722.

(7) Xu, Z.; Han, S.; Gu, Z.; Wu, J. Advances and impact of antioxidant hydrogel in chronic wound healing. *Adv. Healthcare Mater.* **2020**, *9*, No. 1901502.

(8) Xiang, J.; Shen, L.; Hong, Y. Status and future scope of hydrogels in wound healing: Synthesis, materials and evaluation. *Eur. Polym. J.* **2020**, *130*, No. 109609.

(9) He, J.; Shi, M.; Liang, Y.; Guo, B. Conductive adhesive self-healing nanocomposite hydrogel wound dressing for photothermal therapy of infected full-thickness skin wounds. *Chem. Eng. J.* **2020**, *394*, No. 124888.

(10) Gao, G.; Jiang, Y. W.; Jia, H. R.; Wu, F. G. Near-infrared light-controllable on-demand antibiotics release using thermo-sensitive hydrogel-based drug reservoir for combating bacterial infection. *Biomaterials* **2019**, *188*, 83−95.

(11) Sang, Y. J.; Li, W.; Liu, H.; Zhang, L.; Wang, H.; Liu, Z. W.; Ren, J. S.; Qu, X. G. Construction of Nanozyme-Hydrogel for Enhanced Capture and Elimination of Bacteria. *Adv. Funct. Mater.* **2019**, *29*, No. 1900518.

(12) Mirani, B.; Pagan, E.; Currie, B.; Siddiqui, M. A.; Hosseinzadeh, R.; Mostafalu, P.; Zhang, Y. S.; Ghahary, A.; Akbari, M. An Advanced Multifunctional Hydrogel-Based Dressing for Wound Monitoring and Drug Delivery. *Adv. Healthcare Mater.* **2017**, *6*, No. 1700718.

(13) Liu, G.; Zhou, Y.; Xu, Z.; Bao, Z.; Zheng, L.; Wu, J. Janus hydrogel with dual antibacterial and angiogenesis functions for enhanced diabetic wound healing. *Chin. Chem. Lett.* **2023**, *34*, No. 107705.

(14) Liang, Y.; Xu, H.; Li, Z.; Zhangji, A.; Guo, B. Bioinspired Injectable Self-Healing Hydrogel Sealant with Fault-Tolerant and Repeated Thermo-Responsive Adhesion for Sutureless Post-Wound-Closure and Wound Healing. *Nano-Micro Lett.* **2022**, *14*, 185.

(15) Akula, S.; Brosch, I. K.; Leipzig, N. D. Fluorinated methacrylamide chitosan hydrogels enhance cellular wound healing processes. *Ann. Biomed. Eng.* **2017**, *45*, 2693−2702.

(16) Patil, P. S.; Fountas-Davis, N.; Huang, H.; Evancho-Chapman, M. M.; Fulton, J. A.; Shriver, L. P.; Leipzig, N. D. Fluorinated methacrylamide chitosan hydrogels enhance collagen synthesis in wound healing through increased oxygen availability. *Acta Biomater.* **2016**, *36*, 164−174.

(17) Ochoa, M.; Rahimi, R.; Zhou, J.; Jiang, H.; Yoon, C. K.; Maddipatla, D.; Narakathu, B. B.; Jain, V.; Oscai, M. M.; Morken, T. J. Integrated sensing and delivery of oxygen for next-generation smart wound dressings. *Microsyst. Nanoeng.* **2020**, *6*, 1−16.

(18) Choi, J.; Hong, G.; Kwon, T.; Lim, J. O. Fabrication of oxygen releasing scaffold by embedding H2O2-PLGA microspheres into alginate-based hydrogel sponge and its application for wound healing. *Appl. Sci.* **2018**, *8*, No. 1492.

(19) Li, Y.; Fu, R.; Duan, Z.; Zhu, C.; Fan, D. Adaptive hydrogels based on nanozyme with dual-enhanced triple enzyme-like activities for wound disinfection and mimicking antioxidant defense system. *Adv. Healthcare Mater.* **2022**, *11*, No. 2101849.

(20) Fu, Y.; Xie, X.; Wang, Y.; Liu, J.; Zheng, Z.; Kaplan, D. L.; Wang, X. Sustained Photosynthesis and Oxygen Generation of Microalgae-Embedded Silk Fibroin Hydrogels. *ACS Biomater. Sci. Eng.* **2021**, *7*, 2734−2744.

(21) Chen, H.; Cheng, Y.; Tian, J.; Yang, P.; Zhang, X.; Chen, Y.; Hu, Y.; Wu, J. Dissolved oxygen from microalgae-gel patch promotes chronic wound healing in diabetes. *Sci. Adv.* **2020**, *6*, No. eaba4311.
(22) Li, W.; Wang, S.; Zhong, D.; Du, Z.; Zhou, M. A bioactive living hydrogel: photosynthetic bacteria mediated hypoxia elimination and bacteria-killing to promote infected wound healing. *Adv. Therapeutics* **2021**, *4*, No. 2000107.
(23) Corrales-Orovio, R.; Carvajal, F.; Holmes, C.; Miranda, M.; González-Itier, S.; Cárdenas, C.; Vera, C.; Schenck, T. L.; Egaña, J. T. Development of a Photosynthetic Hydrogel as Potential Wound Dressing for the Local Delivery of Oxygen and Bioactive Molecules. *Acta Biomater.* **2022**, 154−166.
(24) Jee, J. P.; Pangeni, R.; Jha, S. K.; Byun, Y.; Park, J. W. Preparation and in vivo evaluation of a topical hydrogel system incorporating highly skin-permeable growth factors, quercetin, and oxygen carriers for enhanced diabetic wound-healing therapy. *Int. J. Nanomed.* **2019**, *14*, 5449−5475.
(25) Song, R.; Hu, D.; Chung, H. Y.; Sheng, Z.; Yao, S. Lipid-polymer bilaminar oxygen nanobubbles for enhanced photodynamic therapy of cancer. *ACS Appl. Mater. Interfaces* **2018**, *10*, 36805−36813.
(26) Song, R.; Peng, S.; Lin, Q.; Luo, M.; Chung, H. Y.; Zhang, Y.; Yao, S. pH-responsive oxygen nanobubbles for spontaneous oxygen delivery in hypoxic tumors. *Langmuir* **2019**, *35*, 10166−10172.
(27) Cavalli, R.; Bisazza, A.; Giustetto, P.; Civra, A.; Lembo, D.; Trotta, G.; Guiot, C.; Trotta, M. Preparation and characterization of dextran nanobubbles for oxygen delivery. *Int. J. Pharm.* **2009**, *381*, 160−165.
(28) Cavalli, R.; Bisazza, A.; Rolfo, A.; Balbis, S.; Madonnaripa, D.; Caniggia, I.; Guiot, C. Ultrasound-mediated oxygen delivery from chitosan nanobubbles. *Int. J. Pharm.* **2009**, *378*, 215−217.
(29) Han, X.; Jeong, Y.; Irudayaraj, J. Nanocatalase-Based Oxygen-Generating Nanocarriers for Active Oxygen Delivery to Relieve Hypoxia in Pancreatic Cancer. *ACS Appl. Nano Mater.* **2022**, *5*, 17248−17257.
(30) Batchelor, D. V.; Armistead, F. J.; Ingram, N.; Peyman, S. A.; Mclaughlan, J. R.; Coletta, P. L.; Evans, S. D. Nanobubbles for therapeutic delivery: Production, stability and current prospects. *Curr. Opin. Colloid Interface Sci.* **2021**, *54*, No. 101456.
(31) Messerschmidt, V.; Ren, W.; Tsipursky, M.; Irudayaraj, J. Characterization of Oxygen Nanobubbles and In Vitro Evaluation of Retinal Cells in Hypoxia. *Transl. Vision Sci. Technol.* **2023**, *12*, 16.
(32) Bhandari, P.; Novikova, G.; Goergen, C. J.; Irudayaraj, J. Ultrasound beam steering of oxygen nanobubbles for enhanced bladder cancer therapy. *Sci. Rep.* **2018**, *8*, No. 3112.
(33) Bhandari, P.; Wang, X.; Irudayaraj, J. Oxygen nanobubble tracking by light scattering in single cells and tissues. *ACS Nano* **2017**, *11*, 2682−2688.
(34) Owen, J.; McEwan, C.; Nesbitt, H.; Bovornchutichai, P.; Averre, R.; Borden, M.; McHale, A. P.; Callan, J. F.; Stride, E. Reducing tumour hypoxia via oral administration of oxygen nanobubbles. *PLoS One* **2016**, *11*, No. e0168088.
(35) Bhandari, P. N.; Cui, Y.; Elzey, B. D.; Goergen, C. J.; Long, C. M.; Irudayaraj, J. Oxygen nanobubbles revert hypoxia by methylation programming. *Sci. Rep.* **2017**, *7*, No. 9268.
(36) Fayyaz, M.; Jabeen, M.; Tsipursky, M. S.; Irudayaraj, J. Dextran-based oxygen nanobubbles for treating inner retinal hypoxia. *ACS Appl. Nano Mater.* **2021**, *4*, 6583−6593.
(37) Mahmoud, R. A.; Hussein, A. K.; Nasef, G. A.; Mansour, H. F. Oxiconazole nitrate solid lipid nanoparticles: formulation, in-vitro characterization and clinical assessment of an analogous loaded carbopol gel. *Drug Dev. Ind. Pharm.* **2020**, *46*, 706−716.
(38) Rahman, S. A.; Abdelmalak, N. S.; Badawi, A.; Elbayoumy, T.; Sabry, N.; El Ramly, A. Tretinoin-loaded liposomal formulations: from lab to comparative clinical study in acne patients. *Drug Delivery* **2016**, *23*, 1184−1193.
(39) Saeedi, M.; Morteza-Semnani, K.; Ghoreishi, M. R. The treatment of atopic dermatitis with licorice gel. *J. Dermatol. Treatment* **2003**, *14*, 153−157.
(40) Kolman, M.; Smith, C.; Chakrabarty, D.; Amin, S. Rheological stability of carbomer in hydroalcoholic gels: Influence of alcohol type. *Int. J. Cosmet. Sci.* **2021**, *43*, 748−763.
(41) Bukowski, R. M.; Ciriminna, R.; Pagliaro, M.; Bright, F. V. High-performance quenchometric oxygen sensors based on fluorinated xerogels doped with [Ru (dpp) 3] 2+. *Anal. Chem.* **2005**, *77*, 2670−2672.
(42) Guan, Y.; Niu, H.; Liu, Z.; Dang, Y.; Shen, J.; Zayed, M.; Ma, L.; Guan, J. Sustained oxygenation accelerates diabetic wound healing by promoting epithelialization and angiogenesis and decreasing inflammation. *Sci. Adv.* **2021**, *7*, No. eabj0153.
(43) Microbiology and Sterility Assurance Committee of the United States Pharmacopeia, Sterility Tests, Rec.. https://www.usp.org/harmonization-standards/pdg/general-methods/sterility-test (accessed 2016-11-16).
(44) Xia, Y. P.; Zhao, Y.; Tyrone, J. W.; Chen, A.; Mustoe, T. A. Differential activation of migration by hypoxia in keratinocytes isolated from donors of increasing age: implication for chronic wounds in the elderly. *J. Invest. Dermatol.* **2001**, *116*, 50−56.
(45) Steinbrech, D. S.; Longaker, M. T.; Mehrara, B. J.; Saadeh, P. B.; Chin, G. S.; Gerrets, R. P.; Chau, D. C.; Rowe, N. M.; Gittes, G. K. Fibroblast response to hypoxia: the relationship between angiogenesis and matrix regulation. *J. Surg. Res.* **1999**, *84*, 127−133.
(46) Kim, J.; Kim, B.; Kim, S. M.; Yang, C. E.; Song, S. Y.; Lee, W. J.; Lee, J. H. Hypoxia-Induced Epithelial-To-Mesenchymal Transition Mediates Fibroblast Abnormalities via ERK Activation in Cutaneous Wound Healing. *Int J Mol Sci* **2019**, *20*, No. 2546.
(47) Zhao, B.; Guan, H.; Liu, J. Q.; Zheng, Z.; Zhou, Q.; Zhang, J.; Su, L. L.; Hu, D. H. Hypoxia drives the transition of human dermal fibroblasts to a myofibroblast-like phenotype via the TGF-beta1/Smad3 pathway. *Int. J. Mol. Med.* **2017**, *39*, 153−159.
(48) Wu, Y.; Zhang, Q.; Ann, D. K.; Akhondzadeh, A.; Duong, H. S.; Messadi, D. V.; Le, A. D. Increased vascular endothelial growth factor may account for elevated level of plasminogen activator inhibitor-1 via activating ERK1/2 in keloid fibroblasts. *Am. J. Physiol. Cell Physiol.* **2004**, *286*, C905−C912.

https://doi.org/10.1021/acsanm.3c01812
ACS Appl. Nano Mater. 2023, 6, 13116−13126